SCIENTIFIC REPORTS

OPEN

SUBJECT AREAS:
SELF-ASSEMBLY
MAGNETO-OPTICS

Received
8 August 2014

Accepted
3 November 2014

Published
21 November 2014

Correspondence and requests for materials should be addressed to M.L. (mtliu@cugb.edu.cn)

Assembly of luminescent ordered multilayer thin-films based on oppositely-charged MMT and magnetic NiFe-LDHs nanosheets with ultra-long lifetimes

Meitang Liu, Tianlei Wang, Hongwen Ma, Yu Fu, Kunran Hu & Chao Guan

Beijing Key Laboratory of Materials Utilization of Nonmetallic Minerals and Solid Wastes, National Laboratory of Mineral Materials, School of Materials Science and Technology, China University of Geosciences, Beijing, 100083.

In this present report, luminescent ordered multilayer thin films (OMFs) based on oppositely-charged inorganic nanosheets and the different oppositely-charged chromophores were fabricated via layer-by-layer assembly method. Exfoliated layered double hydroxides (LDHs) and montmorillonite (MMT) nanosheets with opposite charges can be expected to provide a pseudo electronic microenvironment (PEM) which has not been declared in previous literatures, and transition metal-bearing LDHs nanosheets can offer an additional ferromagnetic effect (FME) for the chromophores at the same time. Surprisingly, the luminescent lifetimes of those OMFs with PEM and FME are significantly prolonged compared with that of the pristine chromophores, even much longer than those of OMFs without oppositely-charged and ferromagnetic architecture. Therefore, it is highly expected that the PEM and FME formed by oppositely-charged and transition metal-bearing inorganic nanosheets have remarkable influence on obtaining better optical property, which suggests a new potential way to manipulate, control and develop the novel light-emitting materials and optical devices.

Layered materials have attracted attentions to their rich fundamental physics and potential applications in future multifunctional devices, and the nanosheets of those have been used as building units for making new designed organic-inorganic or inorganic-inorganic nanomaterials due to their intrinsic unique two-dimensional structure[1–7]. LDHs and MMT, the inorganic layered minerals containing ionic nanosheets, have partially been widely applied in sensing, catalysis and energy storage *etc*[8–13]. As the successful liquid exfoliation of layered materials and the fruitful assembly of the inorganic nanosheets with polyelectrolyte, other different inorganic nanosheets, even quantum dots and so on[14–21], layer-by-layer assembly method has been masterly used to build layered and ordered functional materials. Transition metal-bearing LDHs are known to have broader technological applications attributing to their special catalytic, electronic, optical, and magnetic properties[22–28]. Specially, Sasaki *et al.* confirmed that transition metal-bearing LDHs' nanosheets can act as nanoscale ferromagnetic layers at room temperature, and their multilayer assemblies exhibited significant magneto-optical response[29]. On the other hand, Liu *et al.*[30] utilized PVA as intermediate linkers to obtain uniform multilayer films (MMT/PVA/CoAl-LDHs/PVA)$_n$, and other scientists successfully fabricated the nano-dimensional hybrid materials with homogeneously precipitation of ionic nanosheets on the oppositely-charged nanosheets' surface via a simple hydrothermal process[31–34]. But there is no relational reports that oppositely-charged nanosheets can be expected to form a PEM between the interlayer, and how the PEM affects the functional molecules in it.

Organic luminescent materials, imputed to their chemical stability and excellent luminescence properties, give rise to many possible applications in chemical sensors, optical devices, photovoltaic cells *etc*[35–37]. But attempts to implement this idea have been hampered by their poor optical stabilities and relatively short service lifetime. Many scientists tried changing the external factors such as thermal and mechanical stimuli, to modify chemical structure of molecules for luminescent materials, thus improve the optical properties[38–41]. Recently, organo-erbium systems, a potential organic optical amplifier material, combined a relatively longer fluorescence lifetime

to produce a medium with exceptional sensitization[42]. Especially, Duan's group successfully utilized non-magnetic LDHs nanosheets assemble well-oriented photoemissive quantum well structures in order to suppress the chromophores' π-π stacking[43–48]. Herein, what we are most interested in are whether organic luminescent materials can be intercalated into the oppositely-charged MMT and magnetic NiFe-LDHs nanosheets, and how the PEM and FME affect the optical properties.

In this work, in order to confirm the universality of the PEM and FME's contribution on the different series chromophores, two kinds of chromophores with opposite charge, a photoactive divalent cationic bis(*N*-methylacridinium) (BNMA) and a luminescent π-conjugated anionic polymer poly [5-methoxy-2-(3-sulfopropoxy)-1,4-phenylenevinylene] potassium (APPV), were assembled with the NiFe-LDHs nanosheets and MMT nanosheets to fabricate series luminescent ordered multilayer thin films, respectively. In the nano-architecture, as the assembled PEM can provide the electronic field in nano-level system and the NiFe-LDHs can offer a constant FME to the chromophores (Figure 1), the OMFs exhibit remarkable optical properties with reasonably longer luminescent lifetimes. Herein, in this work, not only does we successfully fabricate the OMFs with PEM and FME' architecture, which can promote the hybrid systems with various optical functions, but also puts forward a new concept about the PEM and FME' effects on chromophores firstly.

Results

Characterization of luminescent OMFs based on ferromagnetic NiFe-LDHs containing photoactive divalent cations. The growths of $(NiFe\text{-}LDHs/BNMA@PVA)_n$ OMFs by UV-vis absorption spectra were measured after different deposition cycles (Figure 2a), and the intensities of the characteristic absorption bands of BNMA at 264.0 nm and 371.5 nm correlate linearly with the number of deposition cycles (Figure 2a, inset), demonstrating a stepwise and regular growth procedure. Furthermore, the fluorescence emission intensity at 508 nm displays a consistent increase with the number of deposition cycles, as shown in Figure 2b, and no obvious red or blue shifts occur compared with the pristine BNMA powders, suggesting there is no formation of BNMA aggregation throughout the whole assembly processing. This can also be visualized by irradiating the thin films under daylight and UV light (365 nm), respectively (Figure 2c), where these films exhibit uniform enhanced luminescence with increasing the number of deposition cycles. The $(NiFe\text{-}LDHs/BNMA@PVA)_n$ OMFs surface is microscopically smooth and uniform,according to the top view of the SEM image (Figure 2d). Moreover, the side view of the SEM image (Figure 2d, inset) show that OMFs are continuous and homogeneous, with the obvious layer structure. Furthermore, small angle XRD peaks intensities of the as-prepared OMFs increasing with the layer number indicate that the OMFs are assembled by a stepwise and regular growth procedure with a period of *ca.* 4.7 nm (Figure 2e). Above all, the OMFs exhibit an ordered and regular film growth procedure and uniform enhanced luminescence as the number of deposition cycles increasing.

In order to verify the effect of NiFe-LDHs nanosheets' ferro-magnetism, the OMFs were studied by detecting luminescent lifetimes (Figure 2f). Surprisingly, it is amazing that the luminescent lifetimes of $(NiFe\text{-}LDHs/BNMA@\ PVA)_n$ OMFs (12.75–13.85 ns) are prolonged nearly 3-fold compared with the $(MgAl\text{-}LDHs/BNMA@\ PVS)_n$ OMFs (4.61–4.88 ns), and are also amazingly prolonged about 37-fold compared with the pristine powder BNMA (0.37 ns)[47]. The profound increasing is partially ascribed to the isolation effect imposed by the rigid NiFe-LDHs nanosheets, preventing the formation of BNMA aggregation. But most importantly, NiFe-LDHs can offer a constant FME, thus definitely prolonging their luminescent lifetimes. Above all, FME is beneficial to obtain better photoemission behavior in the OMFs system.

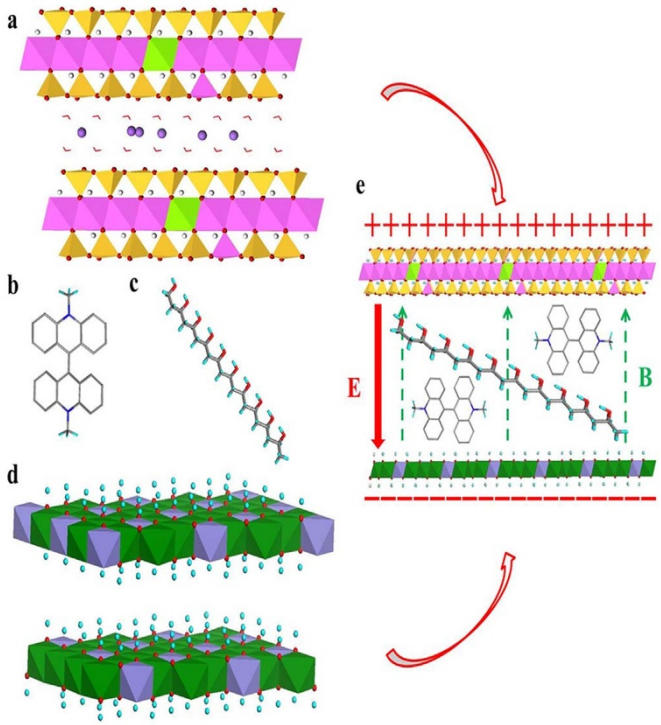

Figure 1 | (a) A representation of MMT, (b) Structure of APPV (c) Structure of PVA Chemical formula of APPV, (d) A representation of NiFe-LDHs, (e) The assembly of OMFs with the PEM and MFE. pink: aluminum element, green: magnesium element, yellow: silicon element, dark green: nickel element, purple: iron element.

Characterization of luminescent OMFs with PEM and FME containing photoactive divalent cations. The UV-visible absorption spectra of $(MMT/BNMA@PVA/NiFe\text{-}LDHs/BNMA@PVA)_n$ OMFs with varying numbers of assembly steps are shown in Figure 3a, and a linear increase in absorbance at 264.0 nm or 371.5 nm was observed upon increasing the number of bilayers (Figure 3a, inset). Furthermore, the fluorescence emission intensity at 508 nm and photos under daylight and UV light (365 nm) of these films display uniform enhanced luminescence increasing with the number of deposition cycles, as shown in Figure 3b and 3c. SEM images (Figure 3d) shows that the films are so smooth, continuous and homogeneous and XRD patterns show that the OMFs are significantly ordered and grow with a period of *ca.* 7.4 nm (Figure 3e). Hence, the OMFs, with an ordered and regular structure and uniform enhanced yellow-green luminescence as the number of deposition cycles increasing, can be obtained.

In order to univocally attribute PEM's contribution, the OMFs were studied by detecting luminescent lifetimes, as shown in Figure 3f. Meaningfully, it is amazing that the luminescent lifetimes of $(MMT/BNMA@PVA/NiFe\text{-}LDHs/BNMA@PVA)_n$ OMFs (15.38–16.52 ns) are extended more than 3-fold compared with the $(MgAl\text{-}LDHs/BNMA@PVS)_n$ OMFs (4.61–4.88 ns), are amazingly prolonged nearly 45-fold compared with the pristine BNMA powders (0.37 ns)[47], and also significantly present a gradient growth compared with the $(NiFe\text{-}LDHs/BNMA@PVA)_n$ OMFs. The profound increasing is partially due to the negative-charged MMT nanosheets' electrostatic attraction to BNMA and the isolation effect imposed by the rigid LDHs and MMT nanosheets, preventing the formation of BNMA aggregation. What's more, positive charged NiFe-LDHs and negative charged MMT nanosheets can form PEM and NiFe-LDHs is able to offer a constant FME, which will constrain the electron vibration in the conjugate structure of chromophores definitely, thus prolonging their luminescent lifetimes.

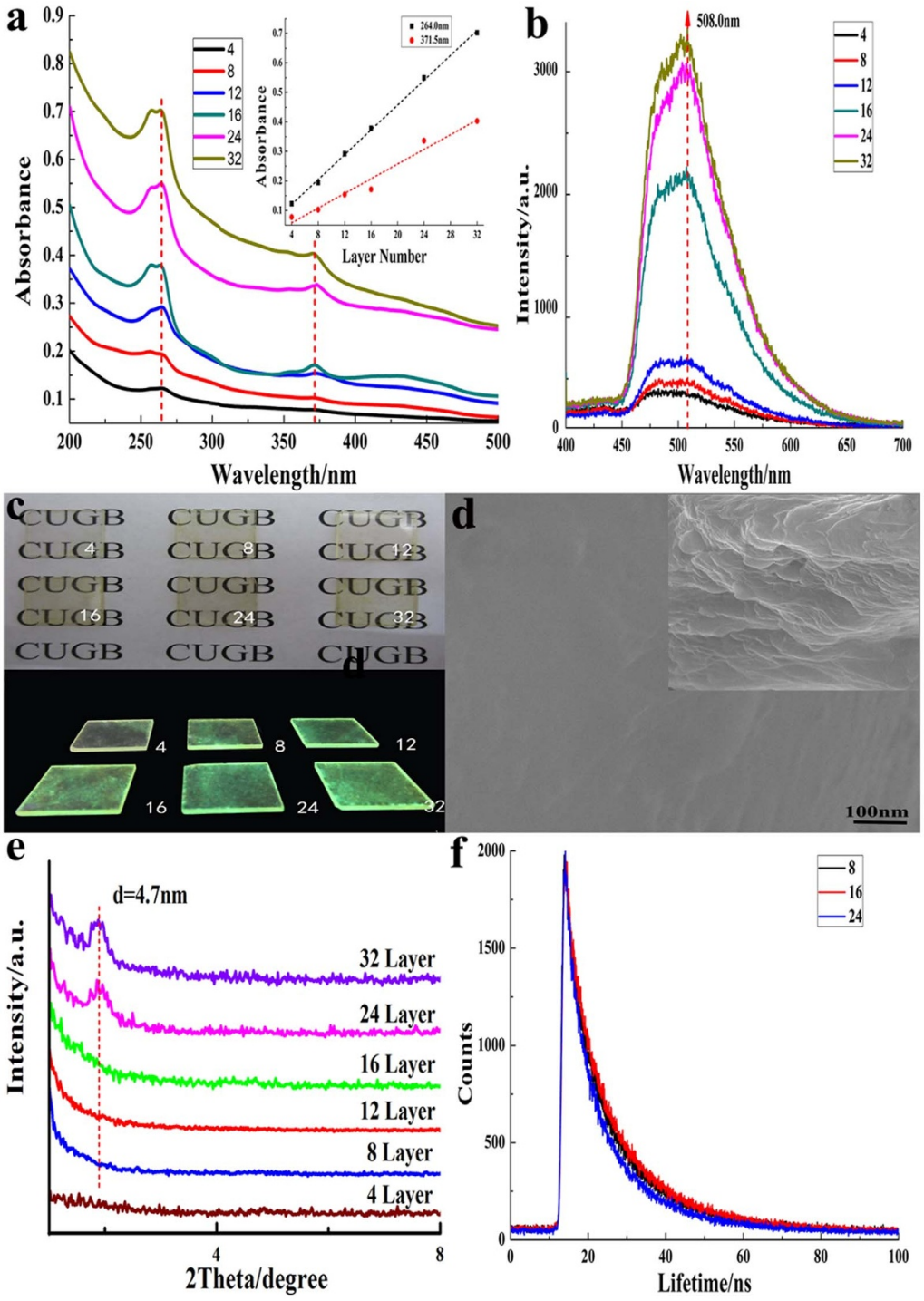

Figure 2 | Characterization of (NiFe-LDHs/BNMA@PVA)$_n$ OMFs (a) UV-visible absorption spectra, the inset shows the absorbance increasing linear relationship in 264.0 nm and 371.5 nm. (b) Photoluminescence spectra. (c) Photographs of OMFs with different bilayer numbers under daylight and UV light (365 nm), respectively. (d) The top view of the SEM image, the inset shows the side view of the SEM image. (e) Small angle XRD patterns. (f) Fluorescence decay profiles.

Above all, the PEM and FME can signally prolong the luminescent lifetimes, simultaneously.

Characterization of luminescent OMFs based on ferromagnetic NiFe-LDHs containing luminescent π-conjugated anionic polymer. In order to confirm the universality of the novel concept for more series chromophores, we selected a luminescent π-conjugated anionic polymer APPV to assemble the luminescent OMFs. The UV-visible absorption spectra of (NiFe-LDHs/APPV@PVA)$_n$ OMFs with varying numbers of assembly steps are shown in Figure 4a, and the intensities of absorption peaks exhibit correlate linearly with the number of deposition cycles (Figure 4a, inset). Furthermore, the fluorescence emission intensity also displays a consistent increase with deposition cycles, as shown in Figure 4b, and photos of these films under daylight and UV light (365 nm) (Figure 4c) exhibit uniform enhanced luminescence with increasing *n*. SEM image (Figure 4d) and XRD patterns (Figure 4e) show that the film surface is smooth, continuous and homogeneous,

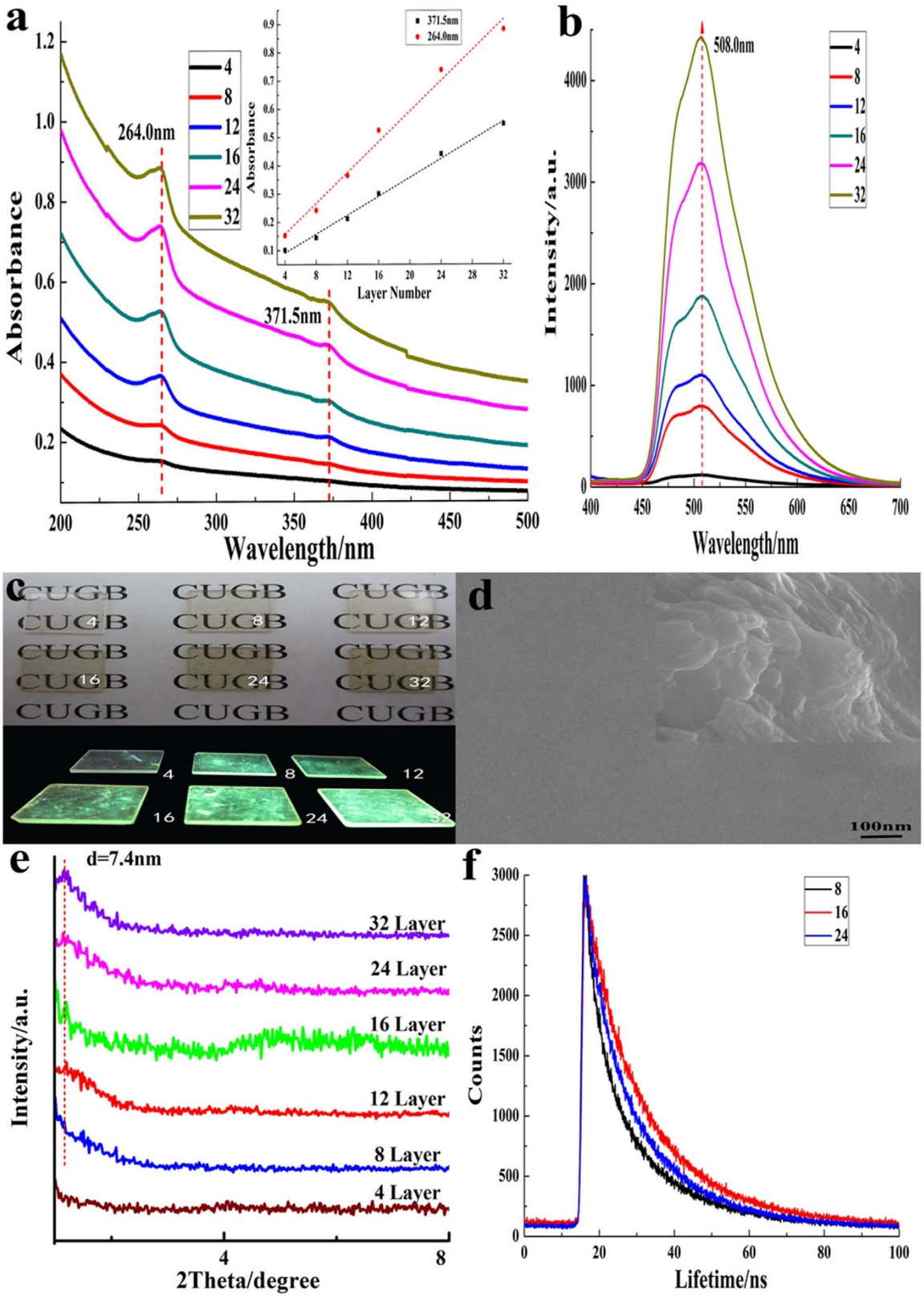

Figure 3 | Characterization of $(MMT/BNMA@PVA/NiFe\text{-}LDHs/BNMA@PVA)_n$ OMFs (a) UV-visible absorption spectra, the inset shows the absorbance increasing linear relationship in 264.0 nm and 371.5 nm. (b) Photoluminescence spectra. (c) Photographs of OMFs with different bilayer numbers under daylight and UV light (365 nm), respectively. (d) The top view of the SEM image, the inset shows the side view of the SEM image. (e) Small angle XRD patterns. (f) Fluorescence decay profiles.

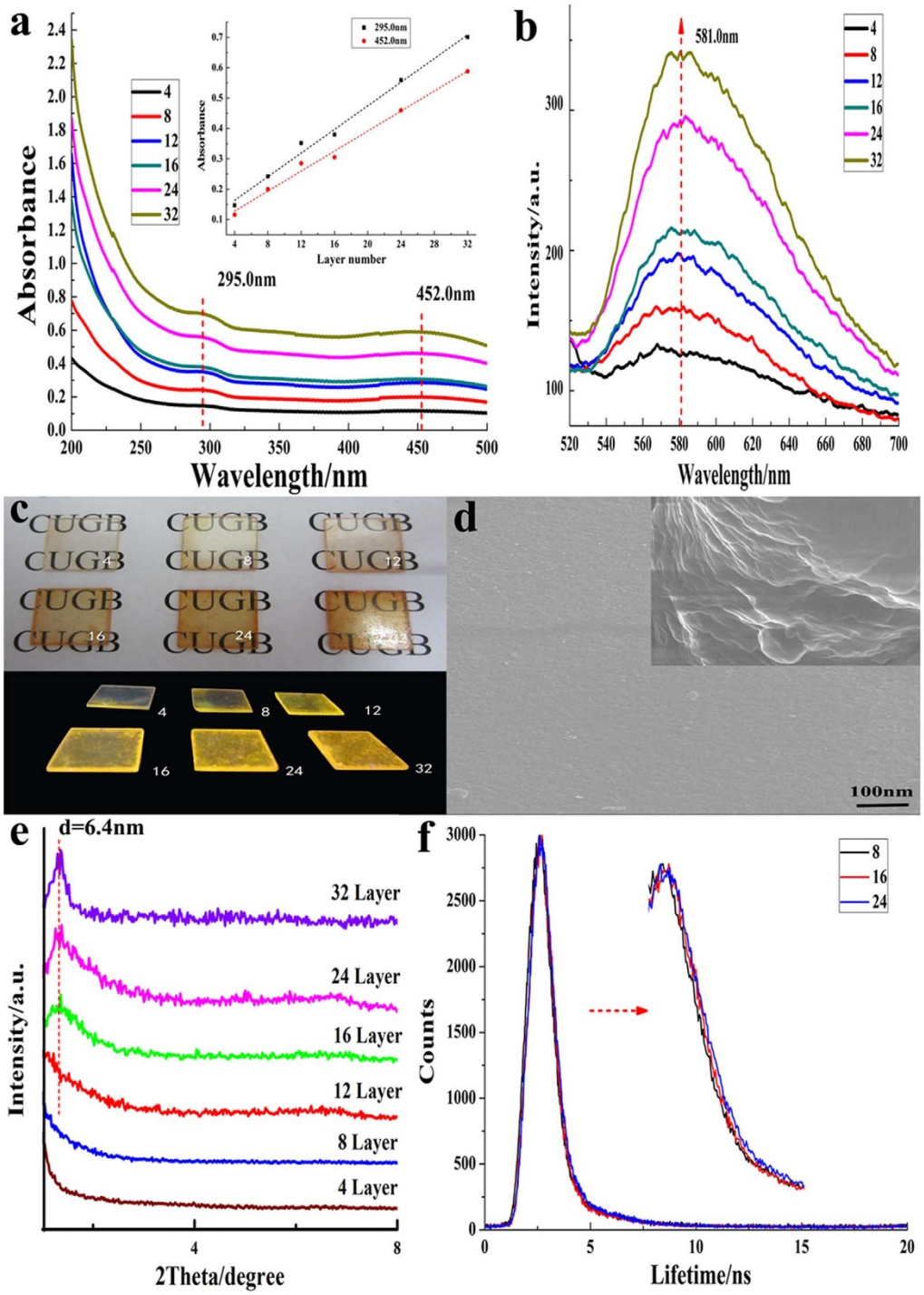

Figure 4 | Characterization of $(NiFe\text{-}LDHs/APPV@PVA)_n$ OMFs (a) UV-visible absorption spectra, the inset shows the absorbance increasing linear relationship in 295.0 nm and 452.0 nm. (b) Photoluminescence spectra. (c) Photographs of OMFs with different bilayer numbers under daylight and UV light (365 nm), respectively. (d) The top view of the SEM image, the inset shows the side view of the SEM image. (e) Small angle XRD patterns. (f) Fluorescence decay profiles.

growing with a period of ca. 6.4 nm. Above all, the OMFs exhibit an ordered and regular film growth procedure and uniform enhanced yellow luminescence as the deposition cycles increasing.

It is amazing that the luminescent lifetimes of $(NiFe\text{-}LDHs/APPV@PVA)_n$ OMFs (1.26–1.38 ns) (Figure 4f) are about 1.5 times as long as $(MgAl\text{-}LDHs/APPV)_n$ OMFs' (0.66–0.81 ns),and are also amazingly 2.3 times the size of the pristine APPV solution's (0.60 ns)[48]. This remarkable increase is partially related to the uniform dispersion of the APPV anion between NiFe-LDHs nanosheets, with the existence of PVA polyanions. But the critical and important reason is that NiFe-LDHs can offer a constant FME, which affect the conjugate structure's electron cloud of chromophores, thus definitely prolonging their luminescent lifetimes. Above all, FME is beneficial to obtain better photoemission behavior in the OMFs system containing the luminescent π-conjugated anionic polymer.

Characterization of luminescent OMFs with PEM and FME containing luminescent π-conjugated anionic polymer. In order to univocally attribute PEM's contribution to the π-conjugated anionic polymer, we also assemble the OMFs containing APPV

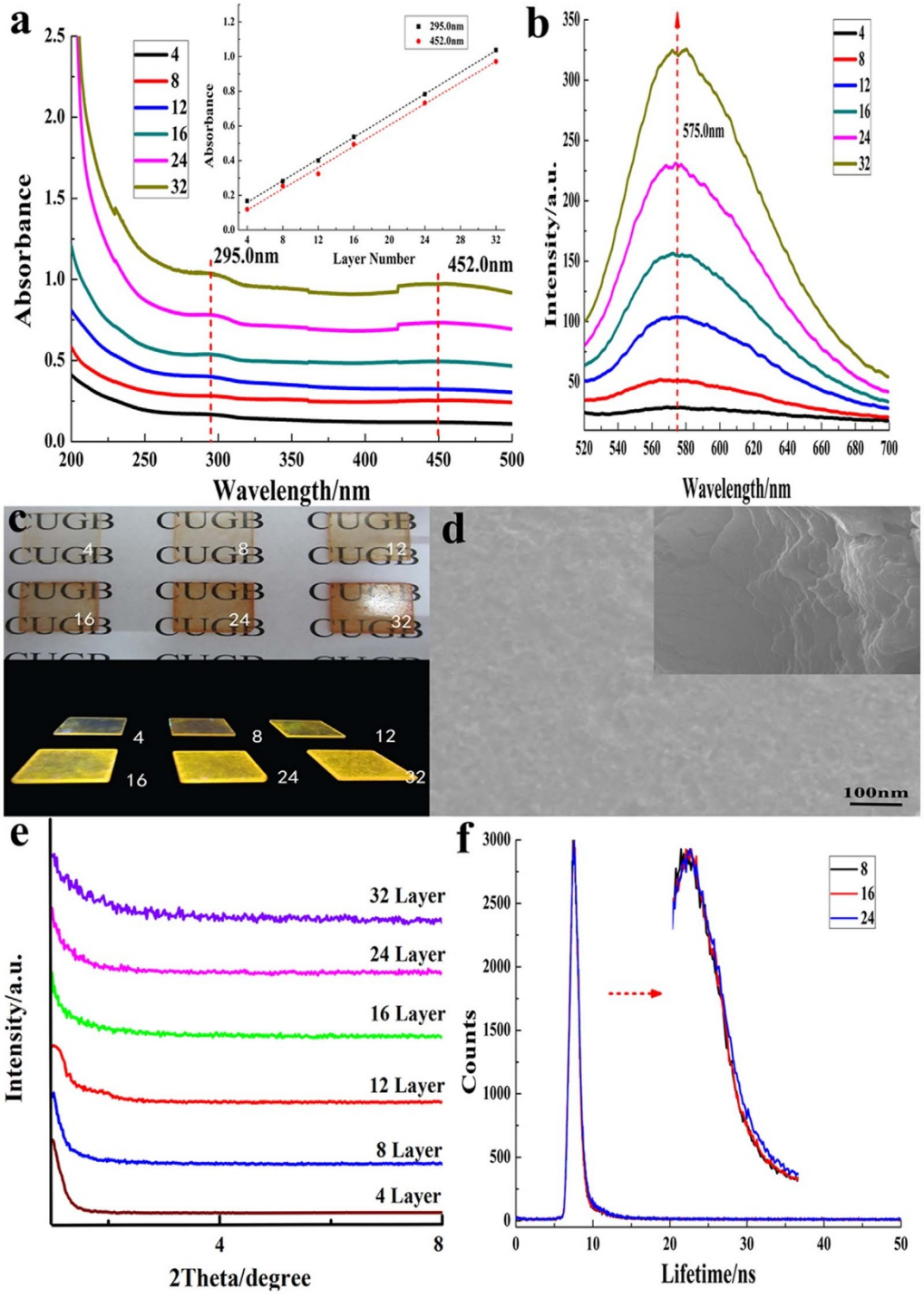

Figure 5 | Characterization of $(MMT/APPV@PVA/NiFe\text{-}LDHs/APPV@PVA)_n$ OMFs (a) UV-visible absorption spectra, the inset shows the absorbance increasing linear relationship in 295.0 nm and 452.0 nm. (b) Photoluminescence spectra. (c) Photographs of OMFs with different bilayer numbers under daylight and UV light (365 nm), respectively. (d) The top view of the SEM image, the inset shows the side view of the SEM image. (e) Small angle XRD patterns. (f) Fluorescence decay profiles.

based on NiFe-LDHs and MMT nanosheets. The UV-visible absorption spectra of $(MMT/APPV@PVA/NiFe\text{-}LDHs/APPV@PVA)_n$ OMFs with varying numbers of assembly steps are shown in Figure 5a, and linear increases in absorbance at 295.0 nm and 452.0 nm were observed upon increasing the number of deposition cycles (Figure 5a, inset), the fluorescence emission intensity also displays a consistent increase with the number of deposition cycles, as shown in Figure 5b, and photos of these films exhibit uniform enhanced luminescence with increasing n under daylight and UV light (365 nm) (Figure 5b). SEM image (Figure 4d) show that the film surface is smooth, uniform, continuous and homogeneous, but small angle XRD have no peak, which verify the

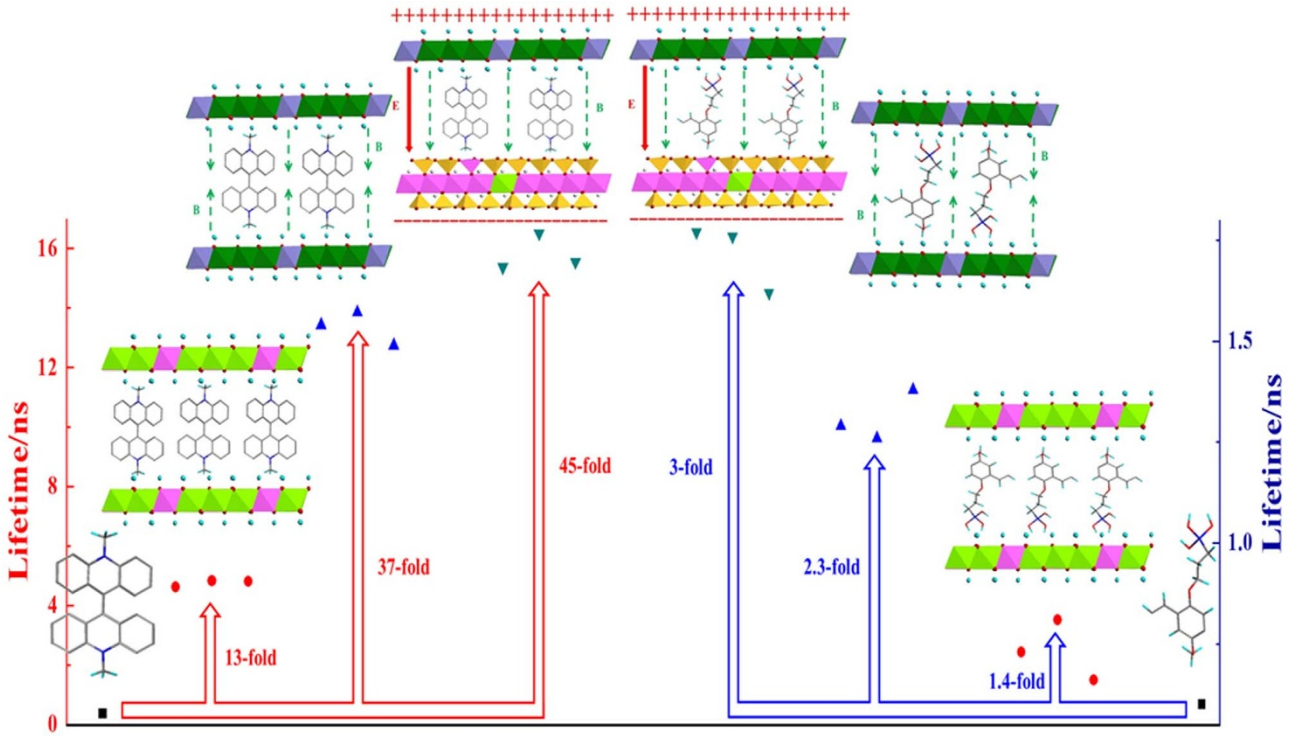

Figure 6 | The comparison of BNMA and APPV' lifetimes under the different environments. Black dots represent the luminescent lifetimes of pristine BNMA or APPV, the red stand for the lifetimes of $(MgAl\text{-}LDHs/BNMA@PVS)_n$ OMFs or $(MgAl\text{-}LDHs/APPV)_n$ OMFs, and the blue show the luminescent lifetimes of $(NiFe\text{-}LDHs/BNMA@PVA)_n$ OMFs or $(NiFe\text{-}LDHs/APPV@PVA)_n$ OMFs. The dark green stand for the luminescent lifetimes of $(MMT/BNMA@PVA/NiFe\text{-}LDHs/BNMA@\ VA)_n$ OMFs or $(MMT/APPV@PVA/NiFe\text{-}LDHs/APPV@PVA)_n$ OMFs.

interlayer spacing are enough large. Hence, the OMFs, with an ordered and regular structure and uniform enhanced yellow luminescence as the number of deposition cycles increasing, can be obtained.

Wondrously, it is amazing that the luminescent lifetimes of $(MMT/APPV@PVA/NiFe\text{-}LDHs/APPV@PVA)_n$ OMFs (1.62–1.77 ns) are extended approximate 2.3-fold compared with the $(MgAl\text{-}LDHs/APPV)_n$ OMFs (0.66–0.81 ns), are amazingly increased more than 3-fold compared with the pristine APPV solution (0.60 ns)[48], and are also significantly multiplied by 1.3 times of the $(NiFe\text{-}LDHs/APPV@PVA)_n$ OMFs', as shown in Figure 5f. The prominent increasing is partially referred to the negative-charged LDHs nanosheets' electrostatic attraction to APPV and the isolation effect imposed by the rigid LDHs and MMT nanosheets, preventing the formation of APPV aggregation. But most dominantly, oppositely-charged NiFe-LDHs and MMT nanosheets can form PEM and NiFe-LDHs is able to offer a FME, which affect the conjugate structure's electron cloud of chromophores, thus definitely prolonging their luminescent lifetimes. According to this remarkable increase, the theory, as mentioned above, that PEM and FME can definitely prolong chromophores' luminescent lifetimes is verified.

Discussion

To sum up, this work assembled series of novel luminescent OMFs containing cationic BNMA or anionic APPV *via* layer-by-layer assembly method. Importantly, the chromophores were successfully confined in the oppositely-charged and ferromagnetic inorganic layer hosts, and it is demonstrated that the PEM and FME are fairly beneficial to enhancing the lifetimes of OMFs through apparently constraining electron vibration in the conjugate structure of chromophores, finally prolonging their luminescent lifetimes. As shown in Figure 6, we compared the lifetimes of BNMA and APPV under the different environments (the pristine, the nonmagnetic LDHs' isolation, FME plus the LDHs' isolation, and PEM, FME plus the LDHs' and MMT' isolation). As introducing the different effect from the inorganic nanosheets, the significant growth presents a regular three-step. The first step is because that the rigid LDHs nanosheets isolation can eliminate the interlayer π-π stacking interaction, as confirmed by Duan *et al*[47,48]. The next conspicuous step is caused by transition metal-bearing LDHs nanosheets can offer FME which can affect the spinning of electron, thus extending the lifetimes. The last noteworthy step is partially due to the initiate MMT nanosheets isolation, but the crucial reason is that the PEM formed by oppositely-charged LDHs and MMT nanosheets, which can definitely impact electron vibration in the conjugate structure of chromophores. In this nano-system, the PEM and FME can influence the variations in the electronic structure, such as increasing in electronic π*-π transition energy and oscillator strength, thus impact the relaxation times of the electron spins, finally prolonging the lifeitmes[49–54]. Above all, PEM and FME are fairly beneficial to obtain better photoemission behavior in the OMFs system.

Therefore, the as-fabricated OMFs are expected to have much flexibility and be potential for manipulating, controlling and developing novel optoelectrical, optomagnetic, even photomagnetoelectric devices. Further work is ongoing with the research on lifetime of various luminescent guests imbedded in series of different layered inorganic nanosheets with PEM and FME.

Methods

Reagents and materials. All the chemicals are analytical grade and used as received without further purification. Bis(N-methylacridinium) (BNMA MW=510.50) and poly[5-methoxy-2-(3-sulfopropoxy)-1,4-phenylenevinylene] potassium salt solution(APPV, 0.25 *wt*% in H_2O) were purchased from Sigma Chemical. *Co. Ltd*, and polyvinyl alcohol (PVA, DP=1750 ± 50) was purchased from Tianjin Fuchen Chemical Reagent Plant. Na-montmorillonite (MMT) was purchased from Zhejiang Sanding *Co. Ltd*. $Ni(NO_3)_2{\cdot}6H_2O$, $Fe(NO_3)_3{\cdot}9H_2O$ were all supplied by the Xilong Chemical Plant. NaOH, $NH_3{\cdot}H_2O$, H_2O_2 (30%), H_2SO_4 (95%–98%) was supplied by Beijng Chemical Reagent Company.

Characterization. UV-visible absorption spectra were measured in the range from 200 to 500 nm on a TU-1901 Double beam UV-vis spectrophotometer with slit width of 5.0 nm. The fluorescence spectra were performed on F-4600 Fluorospectrophotometer. The fluorescence decays measurements of OMFs were recorded by using an Edinburgh Instruments' Steady and transient time-resolved fluorescence spectrometer. X-ray diffraction patterns were recorded using a Rigaku 2500 VB2+PC diffractometer under the conditions: 40 kV, 50 mA. The morphology of thin films was investigated by using a scanning electron microscope (SEMHitachi S-3500), and the accelerating voltage applied was 20 kV. The morphology of layered double hydroxides was investigated by using a transmission electron microscope (Hitachi H9000).

Synthesis of NiFe-LDHs. The NiFe-LDHs was prepared via hydrothermal coprecipitation method. Typically, $Ni(NO_3)_2{\cdot}6H_2O$, $Fe(NO_3)_3{\cdot}9H_2O$ were dissolved in 50 mL boiled deionized water to form a mixed salts solution with the final concentrations of 0.8 and 0.4 mol/L, respectively. The solution of sodium hydroxide (50 mL, 2.4 mol/L) is mixed with the salts solution under vigorous stirring. Then the suspension was stirred at 80°C for 24 h under nitrogen gas flow. The precipitate was centrifuged, washed with hot deionized water and dried in a vacuum at 60°C for 12 h.

Exfoliated of NiFe-LDHs and MMT. The unilamellar, positively charged LDHs nanosheets were obtained by vigorously agitating 0.1 g NiFe-LDHs in 100 mL formamide at room temperature under a N_2 gas flow for 2 days. The MMT powder (1 g) was dissolved in 1000 mL of distilled water. After vigorous stirring for 4 weeks, the upper suspensions with exfoliated MMT nanosheets were obtained after centrifugation at 10000 rpm for 10 min.

Fabrication of $(NiFe\text{-}LDHs/BNMA@PVA)_n$ OMFs and $NiFe\text{-}LDHs/APPV@PVA)_n$ OMFs. The quartz slide (1.5 × 1.5 cm^2) was first cleaned in the solution ($NH_3{\cdot}H_2O : H_2O_2 = 7:3$), then cleaned with H_2SO_4 for 30 min, and finally rinsed and washed thoroughly with deionized water. PVA was dissolved in distilled water to obtain 1wt% aqueous solution, the BNMA (0.1 g) was dissolved in 100 mL deionized water, and then the solution of BNMA and PVA were mixed (1 : 1 in volume) to form BNMA@PVA solution in which the concentration of BNMA is 0.5 g/L. $(NiFe\text{-}LDHs/BNMA@PVA)_n$ OMFs were fabricated by depositing alternatively through LDHs nanosheets solution and BNMA@PVA solution for *n* cycles. The resulting films were dried with a nitrogen gas flow for 2 min. Fabrication of $(NiFe\text{-}LDHs/APPV@PVA)_n$ OMFs was similar with that of $(NiFe\text{-}LDHs/BNMA@PVA)_n$ OMFs.

Fabrication of OMFs $(MMT/BNMA@PVA/NiFe\text{-}LDHs/BNMA@PVA)_n$ and $(MMT/APPV@\ PVA/NiFe\text{-}LDHs/APPV@PVA)_n$ OMFs. Quartz slides (1.5×1.5 cm^2) were cleaned in a "piranha" solution ($H_2SO_4 : H_2O_2 = 3:1$ in volume), and then thoroughly rinsed with distilled water and dried under nitrogen flow. PVA was dissolved in distilled water to obtain 1*wt*% aqueous solution, the BNMA (0.1 g) was dissolved in 100 mL deionized water, and then the solution of BNMA and PVA were mixed (1 : 1 in volume) to form BNMA@PVA solution in which the concentration of BNMA is 0.5 g/L. The $(MMT/BNMA@PVA/NiFe\text{-}LDHs/BNMA@PVA)_n$ OMFs were fabricated by applying a cyclic repetition of the following steps: a) dipping the quartz slide into MMT solution for 5 min, then thoroughly rinsing it with distilled water and drying it; b) dipping it into BNMA@PVA solution for 5 min, then thoroughly rinsing and drying it; c) dipping it into exfoliated NiFe-LDHs suspension for 5 min, then rinsing and drying it; d) dipping it into BNMA@PVA solution for 5 min, then followed by distilled water washing and drying it. All these procedures were repeated n times to produce OMFs of $(MMT/BNMA@PVA/NiFe\text{-}LDHs/BNMA@PVA)_n$ OMFs. Fabrication of $(MMT/APPV@PVA/NiFe\text{-}LDHs/APPV@PVA)_n$ OMFs was similar with that of $(MMT/BNMA@PVA/NiFe\text{-}LDHs/BNMA@PVA)_n$ OMFs.

1. Liu, M. Z., Johnston, M. B. & Snaith, H. J. Efficient Planar Heterojunction Perovskite Solar Cells by Vapour Deposition. *Nature* **50**, 395 (2013).
2. Hodes, G. Perovskite-Based Solar Cells. *Science* **342**, 317 (2013).
3. Ou, X. W. *et al.* π-Conjugated Molecules Crosslinked Graphene-Based Ultrathin Films and Their Tunable Performances in Organic Nanoelectronics. *Adv. Funct. Mater.* **24**, 543 (2014).
4. Wongariyakawee, A., Sch€aeffel, F., Warnerb, J. H. & O'Hare, D. Surfactant Directed Synthesis of Calcium Aluminum Layered Double Hydroxides Nanoplatelets. *J. Mater. Chem.* **22**, 7751 (2012).
5. Wang, L. Z. *et al.* Fabrication and Characterization of Multilayer Ultrathin Films of Exfoliated MnO_2 Nanosheets and Polycations. *Chem. Mater.* **15**, 2873 (2003).
6. Yoo, D. Y. *et al.* Graphene Oxide Nanosheet Wrapped White-Emissive Conjugated Polymer Nanoparticles. *ACS-nano* **8**, 4248 (2014).
7. Parka, D. H., Hwang, S. J., Oh, J. M., Yang, J. H. & Choy, J. H. Polymer-inorganic supramolecular nanohybrids for red, white, green, and blue applications. *Prog. Polym. Sci.* **38**, 1442 (2013).
8. Fan, H., Zhu, J. Y., Sun, J. C., Zhang, S. X. & Ai, S. Y. Ag/AgBr/Co–Ni–NO_3 Layered Double Hydroxide Nanocomposites with Highly Adsorptive and Photocatalytic Properties. *Chem. Eur. J.* **19**, 2523 (2013).
9. Li, M. G., Ji, H. Q., Wang, Y. L., Liu, L. & Gao, F. MgFe-Layered Double Hydroxide Modified Electrodes for Direct Electron Transfer of Hemeproteins. *Biosens. Bioelectron.* **38**, 239 (2012).
10. Choy, J. H., Kwak, S. Y., Jeong, Y. J. & Park, J. S. Inorganic Layered Double Hydroxides as Nonviral Vectirs. *Angew. Chem. Int. Ed.* **39**, 4042 (2000).
11. Ikeda, M. *et al.* Montmorillonite-Supramolecular Hydrogel Hybrid for Fluorocolorimetric Sensing of Polyamines. *J. Am. Chem. Soc.* **133**, 1670 (2011).
12. Gong, J. M., Guan, Z. Q. & Song, D. D. Biosensor Based on Acetylcholinesterase Immobilized onto Layered Double Hydroxides for Flow Injection/Amperometric Detection of Organophosphate Pesticides. *Biosens. Bioelectron.* **39**, 320 (2013).
13. Dutta, K. & Pramanik, A. Synthesis of a Novel Cone-Shaped CaAl-Layered Double Hydroxide (LDH): Its Potential Use as a Reversible Oil Sorbent. *Chem. Commun.* **49**, 6427 (2013).
14. Nicolosi, V., Chhowalla, M., Kanatzidis, M. G., Strano, M. S. & Coleman, J. N. Liquid Exfoliation of Layered Materials. *Science* **340**, 1420 (2013).
15. Podsiadlo, P. *et al.* Ultrastrong and Stiff Layered Polymer Nanocomposites. *Science* **318**, 80 (2007).
16. Han, J. B., Lu, J., Wei, M., Wang, Z. L. & Duan, X. Heterogeneous Ultrathin Films Fabricated by Alternate Assembly of Exfoliated Layered Double Hydroxides and Polyanion. *Chem. Commun.* 5188 (2008).
17. Wang, Q. & O'Hare, D. Recent Advances in the Synthesis and Application of Layered Double Hydroxide (LDH) Nanosheets. *Chem. Rev.* **112**, 4124 (2011).
18. Li, L. *et al.* Layer-by-Layer Assembly and Spontaneous Flocculation of Oppositely Charged Oxide and Hydroxide Nanosheets into Inorganic Sandwich Layered Materials. *J. Am. Chem. Soc.* **129**, 8000 (2007).
19. Xu, D. M., Guan, M. Y., Xu, Q. H. & Guo, Y. Multilayer Films of Layered Double Hydroxide/Polyaniline and Their Ammonia Sensing Behavior. *J. Hazard. Mater.* **262**, 64 (2013).
20. Bujdák, J. Layer-by-Layer Assemblies Composed of Polycationic Electrolyte, Organic Dyes, and Layered Silicates. *J. Phys. Chem. C.* **118**, 7152 (2014).
21. Kong, X. G., Rao, X. Y., Han, J. B., Wei, M. & Duan, X. Layer-by-Layer Assembly of Bi-protein/Layered Double Hydroxide Ultrathin Film and its Electrocatalytic Behavior for Catechol. *Biosens. Bioelectron.* **26**, 549 (2010).
22. Zhang, H., Zhang, G. Y., Bi, X. & Chen, X. T. Facile Assembly of a Hierarchical Core@Shell Fe_3O_4@CuMgAl-LDH (Layered Double Hydroxide) Magnetic Nanocatalyst for the Hydroxylation of Phenol *J. Mater. Chem. A* **1**, 5934 (2013).
23. Shao, M. F., Han, J. B., Shi, W. Y., Wei, M. & Duan, X. Layer-by-Layer Assembly of Porphyrin/Layered Double Hydroxide Ultrathin Film and Its Electrocatalytic Behavior for H_2O_2. *Electrochem. Commun.* **12**, 1077 (2010).
24. Xiang, X., Hima, H. I., Wang, H. & Li, F. Facile Synthesis and Catalytic Properties of Nickel-Based Mixed-Metal Oxides with Mesopore Networks from a Novel Hybrid Composite Precursor. *Chem. Mater.* **20**, 1173 (2008).
25. Dong, X. Y., Wang, L., Wang, D., Li, C. & Jin, J. Layer-by-Layer Engineered Co-Al Hydroxide Nanosheets/Graphene Multilayer Films as Flexible Electrode for Supercapacitor. *Langmuir* **28**, 293 (2012).
26. Liang, J. B. *et al.* Topochemical Synthesis, Anion Exchange, and Exfoliation of Co-Ni Layered Double Hydroxides: A Route to Positively Charged Co-Ni Hydroxide Nanosheets with Tunable Composition. *Chem. Mater.* **22**, 371 (2010).
27. Chen, H., Hu, L. F., Chen, M., Yan, Y. & Wu, L. M. Nickel–Cobalt Layered Double Hydroxide Nanosheets for High-performance Supercapacitor Electrode Materials. *Adv. Funct. Mater.* **24**, 934 (2014).
28. Ma, R. Z. *et al.* Synthesis and Exfoliation of Co^{2+}-Fe^{3+} Layered Double Hydroxides: An Innovative Topochemical Approach. *J. Am. Chem. Soc.* **129**, 5257 (2007).
29. Liu, Z. P. *et al.* Synthesis, Anion Exchange, and Delamination of Co-Al Layered Double Hydroxide: Assembly of the Exfoliated Nanosheet/Polyanion Composite Films and Magneto-Optical Studies. *J. Am. Chem. Soc.* **128**, 4872 (2006).
30. Huang, S. *et al.* Heterogeneous Ultrathin Films of Poly (vinyl alcohol)/Layered Double Hydroxide and Montmorillonite Nanosheets via Layer- by-Layer Assembly. *J. Phys. Chem. B.* **113**, 15225 (2009).
31. Yi, D. Q., Yang, R. J. & Wilkie, C. A. Layered Double Hydroxide-Montmorillonite-a New Nano-Dimensional Material. *Polym. Advan. Technol.* **24**, 204 (2013).
32. Li, H. J., Zhu, G., Liu, Z. H., Yang, Z. P. & Wang, Z. L. Fabrication of a hybrid graphene/layered double hydroxide material. *Carbon* **48**, 4391 (2010).
33. Gong, M. *et al.* An Advanced Ni-Fe Layered Double Hydroxide Electrocatalyst for Water Oxidation. *J. Am. Chem. Soc.* **135**, 8452 (2013).
34. Huang, S. *et al.* Immobilization of Co-Al Layered Double Hydroxides on Graphene Oxide Nanosheets: Growth Mechanism and Supercapacitor Studies. *ACS Appl. Mater. Interfaces* **4**, 2242 (2012).
35. Samuel, I. D. W. & Turnbull, G. A. Organic Semiconductor Lasers. *Chem. Rev.* **107**, 1272 (2007).
36. Strassert, C. A. *et al.* Switching On Luminescence by the Self-Assembly of a Platinum(II) Complex into Gelating Nanofibers and Electroluminescent Films. *Angew. Chem. Int. Ed.* **50**, 946 (2011).
37. Allendorf, M. D., Bauer, C. A., Bhakta, R. K. & Houk, R. J. T. Luminescent Metal-Organic Frameworks. Chem. *Soc. Rev.* **38**, 1330 (2009).
38. Niu, Q. L. *et al.* Enhancing the performance of polymer light-emitting diodes by integrating self-assembled organic nanowires. *Adv. Mater.* **20**, 964 (2008).
39. Sagara, Y. & Kato, T. Mechanically Induced Luminescence Changes in Molecular Assemblies. *Nat. Chem.* **1**, 605 (2009).
40. Luo, X. L. *et al.* Reversible Switching of the Emission of Diphenyldibenzofulvenes by Thermal and Mechanical Stimuli. *Adv. Mater.* **23**, 3261 (2011).

41. Mutai, T., Satou, H. & Araki, K. Reproducible On–off Switching of Solid-State Luminescence by Controlling Molecular Packing Through Heat-Mode Interconversion. *Nat. Mater.* **4**, 685 (2005).
42. Ye, H. Q. *et al.* Organo-Erbium Systems for Optical Amplification at Telecommunications Wavelengths. *Nat. Mater.* **13**, 382 (2014).
43. Yan, D. P., Lu, J., Wei, M., Evans, D. G. & Duan X. Recent Advances in Photofunctional Guest/Layered Double Hydroxide Host Composite Systems and Their Applications: Experimental and Theoretical Perspectives. *J. Mater. Chem.* **21**, 13128 (2011).
44. Yan, D. P. *et al.* Heterogeneous Transparent Ultrathin Films with Tunable-Color Luminescence Based on the Assembly of Photoactive Organic Molecules and Layered Double Hydroxides. *Adv. Funct. Mater.* **21**, 2497 (2011).
45. Yan, D. P. *et al.* Layered Host-Guest Materials with Reversible Piezochromic Luminescence. *Angew. Chem. Int. Ed.* **50**, 7037 (2011).
46. Yan, D. P. *et al.* Ordered Poly (p-phenylene)/Layered Double Hydroxide Ultrathin Films with Blue Luminescence by Layer-by-Layer Assembly. *Angew. Chem. Int. Ed.* **48**, 3073 (2009).
47. Yan, D. P. *et al.* A Strategy to the Ordered Assembly of Functional Small Cations with Layered Double Hydroxides for Luminescent Ultra-thin Films. *Chem. Commun.* **46**, 5912 (2010).
48. Yan, D. P. *et al.* Anionic Poly (p-Phenylenevinylene)/Layered Double Hydroxide Ordered Ultrathin Films with Multiple Quantum Well Structure: A Combined Experimental and Theoretical Study. *Langmuir* **26**, 7007 (2010).
49. Park, H. *et al.* Positive-/Negative-, Erasable-/Immobilized-,Mono-/Multi-Color Fluorescence Image Patterning of Molecular-Scale Porous Polymer Film via a Microcontact Printing Method Using Various Chemical Inks. *Macromol. Rapid Commun.* **32**, 360 (2011).
50. Lee, W. E. *et al.* Desilylation Reaction: Correlation with Variations in Microporous Structure, Chain Conformation, and Lamellar Layer Distance. *Macromol. Rapid Commun.* **32**, 1047 (2011).
51. Lee, W. E. *et al.* Fluorescent Actuator Based on Microporous Conjugated Polymer with Intramolecular Stack Structure. *Adv. Mater.* **24**, 5604 (2012).
52. Lee, W. E. *et al.* Fluorescence turn-on response of a conjugated polyelectrolyte with intramolecular stack structure to biomacromolecules. *Chem. Commun.* **49**, 9857 (2013).
53. Han, D. C. *et al.* Environment-Specifi c Fluorescence Response of Microporous, Conformation-Variable Conjugated Polymer Film to Water in Organic Solvents: On-line Real-Time Monitoring in Fluidic Channels. *Macromol. Chem. Phys.* **215**, 1068 (2014).
54. Bigall, N. C., Parak, W. J. & Dorfs, D. Fluorescent, magnetic and plasmonic-Hybrid multifunctional colloidal nano objects. *Nano Today.* **7**, 282 (2012).

Acknowledgments

This work was supported by the National Natural Science Foundation of China (Grant No.:40802013), Key Projects in the National Science & Technology Pillar Program during the Eleventh Five-year Plan Period (Grant No.: 2006BAD10B04), the Fundamental Research Funds for the Central Universities (Grant No.: 2011YXL058).

Author contributions

M.T.L. designed the whole experiment and analyzed the data of the work. He also revised the manuscript critically and approved the final version for submission. T.L.W. did the most of the experiment and drafted the paper. Moreover, he revised the paper with Liu seriously and submitted the final version of paper as well. H. W. M. helped M.T.L. design the research and gave the interpretation of the whole data. Y.F., K.R.H. and C.G. helped to perform the fluorescence decays characterization and analysis of the data. All the authors have read the paper and approved the final version of the paper for submission.

Additional information

Supplementary information accompanies this paper at http://www.nature.com/scientificreports

Competing financial interests: The authors declare no competing financial interests.

How to cite this article: Liu, M. *et al.* Assembly of luminescent ordered multilayer thin-films based on oppositely-charged MMT and magnetic NiFe-LDHs nanosheets with ultra-long lifetimes. *Sci. Rep.* **4**, 7147; DOI:10.1038/srep07147 (2014).